International Journal of Advanced Research in Physical Science (IJARPS)
Volume 10, Issue 3, 2023, PP 19-34
ISSN No. (Online) 2349-7882
www.arcjournals.org

Some Electrodynamics Problems of Modelling the Nucleation and Crystallization

Petro P. Trokhimchuck*

Anatoliy Svidzinskii Department of Theoretical and Computer Physics, Lesya Ukrayinka Eastern European National University, 13 Voly Avenue, 43025, Lutsk, Ukraine.

Corresponding Author:** ***Petro P. Trokhimchuck, *Anatoliy Svidzinskii Department of Theoretical and Computer Physics, Lesya Ukrayinka Eastern European National University, 13 Voly Avenue, 43025, Lutsk, Ukraine.*

Abstract: *Main concepts and methods of electromagnetic modeling nucleation and crystallization are analyzed. It shown, that this problem is connected with procedure of creation the nano- and microstructures. Short historical analysis of this problem is discussed. Corresponding experimental data are represented. Elionic (ion, laser and electron beam) methods of nucleation and crystal growth and other phase transformations are analyzed. It was shown, that these methods are added the thermodynamical methods with microscopic point of view. Possibility and limitations electromagnetic methods of modelling of the processes nucleation and crystallizations are observed.'*

Keywords: *nucleation, crystallization, Relaxed Optics, laser-induced phase transformations, V. Stafeev phason model, cascade model of excitation the chemical bonds in the regime of saturation of excitation, nanostructures, microstructures.*

1. INTRODUCTION

The nucleation concept must be generalizing on other type processes**,** including electromagnetic and pulses [1 – 30].

To expand the methods of obtaining nuclei of various crystallographic modifications, it is advisable to use the methods of elionic technologies [1-10, 13-16, 18, 20-28]. The use of different types of irradiation: ion, electron, and especially laser allows forming nuclei of both structures with a smaller order of symmetry and structures with a higher order of symmetry [1-5]. At the same time, a cascade of structures can be formed as their order of symmetry decreases.

These nucleation theories and models must base on other physical and chemical aspects as thermodynamical. The main role is played by the excitation saturation mode of the corresponding radiation absorption centers and the mechanisms of their non-radiative relaxation, which lead to the required phase transformations [1-5].

V. Stafeev phason model [1, 12] is represented electrostatic theory which takes into account the existing and changing electrostatic state of the compound to form the nuclei of new phases or aggregate states of matter (phases). Therefore, we analyzed this theory and its some applications.

Cascade model of step-on-step excitation of corresponding chemical bonds in the regime of saturation the excitation allow to explain the processes of creation surface and volume laser-induced structures in various solid: from amorphous to crystals, in both directions. At the same time, it is possible to use both schemes of two-dimensional and three-dimensional crystal lattices and their phase diagrams. Energy calculations can be carried out both for chemical bonds and for the coordination numbers of an atom in a crystal lattice. Since we are talking about structural phase changes of a substance, it is advisable to use physicochemical methods of calculation, not quantum mechanical ones. There is no sense in Brillouin zones say, since when new phases are formed, it is different for each phase.

In this case, cascade processes of conversion of radiation energy into matter and, conversely, matter into radiation are of great importance [1-5]. This makes it possible to control the modes of nucleation of new phases both on the surface and in the volume of the irradiated material. In contrast to continuous nucleation and crystallization, in this case we must have irradiation modes with non-radiative relaxation. For ions and electrons, these can be both continuous and pulse irradiation modes, which

allow you to dial in the appropriate integral dose, and for laser irradiation, only pulse. Therefore, we must build models and theories of these processes taking these features into account.

2. MAIN THEORIES AND MODELS

2.1. Vitaliy Stafeev Phason Model

The problem of the creation new phase centers (phasons) is represented in Stafeef model [1, 12]. It is electrostatic theory. Short review of this theory will be analyzed in this chapter.

Experimental data [12] shown that phasons are mono dispersive particles. Its sizes are depended from properties of its matter and environment of its formation. New condenced phase centers may be generated under vaporation, on substrate, in gas or liquid environment and directly in solid state. Under change of chemical compound phasons change its sizes in jumping way. For various matters minimal sizes of phasons are changed from 1 to 20 nm [12]. Nanoparticles with these sizes are observed in soli state. It is structural defects – clusters [12]. In some environment crystallization centers are covered by shell, its form stands more lock-in. Its nanoparticles are analogous to special "atoms" – small bricks of new matter [12]. It may be included in solution, including solid, and created own condensed matter. For objects of little sizes, classical thermodynamical approaches and characteristics (surface energy a.o.) cannot be used. However, must be existed some physical characteristics of matter and environment, which are determined minimal sizes of phasons.

As rule take into account, that nanoparticles are neutral [12]. But investigations in region of phase transitions were shown that new phase centers (phasons) must be have electrical charge. For example [162], between growth ice layer from water may be generated sufficiently great (decathlons and hundreds Volts) difference of electrical potentials. Under phase transitions in liquid crystals great difference of electrical potentials is observed [12].

Atoms is determined the properties of chemical elements, molecules – chemical properties of substance. Must be existed structural unit that determine physical and other properties of condenced phases of substance. Last is depended not only from state of substrate but from its phase. Phasons may be completed from comparatively small numbers of molecules. Some quantitative threshold must be existed. Beginning from this threshold molecular cluster is transformed to thermodynamically stable phasons [12].

One of the important parameter of any phase is electrochemical potential. Therefore on its border with another phase junction difference of electrical potentials, which is stipulated of difference of electrochemical potentials, must be generated. It may be realized only in presence in each with contact phase's electrical charges with opposite signs. Cluster of bound molecules may be thermodynamically stable center of new phase after formation of proper junction difference of potentials only.

Minimal size of phason is determined from condition, that unit electrical charge q in environment with electrical constant ε on its capacity c is provided the generation of necessary junction difference of potentials $\varphi = q/\varepsilon c$. Center of new phase with minimal sizes was called phason [12]. These centers may be having various forms. For simplification of further analysis we allow that center of new phase is spherical capacitor with diameter d_o. For this suggestion [12]:

size of phason – $d_o = 3{,}6/\varepsilon\varphi$, *нм*;

number molecules in phason – $n_f = 10^2\,\pi\rho d_o^3/M$;

mobility – $\mu = \varepsilon\varphi/6\pi\eta = 5{,}3\cdot10^{-7}\,\varepsilon\varphi/\eta$, $cm^2/V\cdot s$;

diffusive coefficient – $D = 4{,}6\cdot10^{-11}\,\varepsilon\varphi T/\eta$, cm^2/s,

where φ in Volts; q in Coulomb; η viscosity in Poissons; N – Avogadro number; T – temperature; M – molecular weight; ρ is density of phason substrate in g/cm^3.

Diameter, mobility and diffusive coefficient of phasons are determined of electric constant of surrounding environment and difference of electrochemical potentials.

Sign of difference of electrochemical potentials is determined the sign of charge of center of new phase. For vacuum and gas, the role of difference of electrochemical potentials has energy of chemical affinity to electron (or proton) atoms and molecules of phason substrate w. For positive sign of affinity to electron

phason charge will be negative, for positive to proton – positive. Knowledge of phason size allow estimating the affinity to electron (proton) its substance or difference of electrochemical potentials phason and substance of basic phase.

Phasons may be creating more large clusters – polyphasons. It must be quantized on sizes $d = nd_o$, where $n = 1, 2, 3 \ldots$.

Scientists from Berkeley laboratory under researches of properties of lead drop in solid crystal of aluminum for $T = 423$ °C are measured that lead drops have discrete sizes really [12].

Relationship to electron in Al $w = 0{,}46$ *eV*, in Pb $w = 1{,}14$ *eV* and difference of energy of relationship is 0,68 *eV*. Proper size aluminum phason is $d = 5{,}3$ *nm*, that is near to observing size of lead drops – 5 *nm*. According to experimental data [20] nanoparticles of lead are repulsed mutually, that with hear point of view couldn't be. In this theory all phasons have alike electrical charge and therefore Coulomb force of repulse are basic in this case. After increasing of phasons sizes energy of deformation of aluminum lattice is increased and lead drops begin be going to in thick group for decreasing of deformation of aluminum crystal, which is corresponded to experimental data [12].

Some data show that phase transitions are sharp, that is to say that transitional region is absented practically. However, other experimental data show that phase transition is fluent under temperature [12]. Phasons of low temperature phase are presented in stable region of high temperature phase and, on the contrary, phasons of high temperature phase are presented in stable region of low temperature phase. Concentration and sizes of phasons are increased under approach to point of phase transition, in which one phase is changed on another phase. For example, in fullerite (C_{60}) for temperature 260 K phase transition: simple cubic lattice – verge central lattice, is realized. Transition is endothermic and realized in thermal region 20-40 K – in this case two phases are coexisted [12].

Estimations of physical characteristics of basic phasons are next.

Phasons of carbons

Atom of carbon C has value of energy of relationship to electron $w = 1{,}263$ *eV* [12]. Minimal size of phason ($d = 2{,}85$ *nm*) practically is considered with minimal size phasons (2,5 *nm*), which are received with help laser sprayer of ultradispersion diamond layers [12]. Average size nanoparticles of diamond, which are received with help of detonating synthesis, is 4,2 *nm* [12]. Minimal size of diamond phasons, which are grown from hydrogen-methane mixture on silicon substrate, is near to 5 nm [12]. Last increasing size is bound with influence of substrate and high temperature of condensation (850°C).

Smut. After incineration of toluene and acetone the appearance of spherical clusters with sizes 15,5 and 24,5 *nm* with charges 2 i 3 *q* are observed. Difference in size is near to 9 *nm*. Elementary phason – cluster with unit charge – must has size ~ 8 – 9 *nm* end energy of relationship ~0,4–0,5 *eV*. These results are confirmed predicted quantized of phason sizes.

Molecule of carbon C_2 has relationship to electron $w = 3{,}39$ *eV* and create phasons with twin number of atoms. All molecules of fullerenes have twin number of atoms too [12]. Size of phason of molecules C_2 in gas environment $d_o = 1{,}06$ *nm* practically is equaled with size stable spherical molecule fullerene-60 ("near to 1 *nm*" [12]). Internal cavity of fullerene has size ~ 0,7 *nm* [12].

Fullerenes with more large number of molecules are less stable and have ellipsoidal form. Therefore, for receiving more large capacity we must have more large number of molecules and sizes. For example, in fullerene C_{84} $d_o = 1{,}12$ *nm* [12]. An inclusion in fullerene of atoms of another materials is changed it electrochemical potential and size. Last fact is observed in experiment [12].

Fullerite. In crystal of fullerenes C_{60} (fullerites) distance between centers of molecules is 1,06 *nm*. In crystal of fullerite with cubic structure for dense packing distance between molecules of C_{60} is equaled 1,006 *nm* [12]. Accounting density of phason material of molecule C_2 is equaled 1,76 g/cm^3 in our model. But density of solid state must be less on account of cavities, which are generated under condensation of spherical phasons. Density of fullerite is 1,65 g/cm^3 [12]; 1,69 g/cm^3 [12]. In this case we have good coordination with accounting data.

Molecule of carbon C_3 has affinity to electron 2,5 *eV*, therefore accounting size of it phason is $d_o = 1{,}44$ *nm* and volume bigger in 2,5 times then volume of phason molecule C_2.

Affinity to electron of molecule of fullerene C_{60} w = 2,57 *eV*, fuleren C_{70} w = 2,69 *eV*. Size of phasons of molecules of fullerenes C_{60} in environment with ε = 1 d_o = 1,4 *nm*. Experimental data –"near to 1,5 *nm*".

Fullerenes in solutions are existed as clusters – polyphasons with number of molecules 6–20 [12], which are created for time ~10^{-6} *s*. Further in time many days it grows to few hundred nanometers, but it are unstable and disintegrate after shaking. Clusters have fractal structure (as pizza) with fractal parameter k = 2,1. Number particles in cluster is $n_f = (d/d_o)^k$ [12]. Absorptive spectrum of fullerenes is depended from composition of solvent.

Size of clusters is depended from chemical composition of solvent. This result is confirmed the diffusive researches [12]. In benzol (ε = 2,28, w = 0,56 *eV*) accounting size of phasons C_{60} 0,78 *nm*, phasons C_{70} d_o = 0,74 *nm*. Experimental data: height 0,78 *nm*, diameter 0,694 *nm* [12]. In CS_2 (ε = 2,28, w = 0,85 *eV*) accounting size of phason C_{60} d_o = 0,79 *nm*; size of phason C_{70} d_o = 0,74 *nm*. Experimental data d_o = 0,357×2=0,71 *nm* [20]. Viscosity of benzol η=6,5×10^{-3} Poissons, therefore diffusive coefficient of fullerenes' must be ~10^{-5} cm^2/s, that near to values of diffusive coefficients in analogous materials [12].

Phasons may be basis for creation structures with quantum dots.

Therefore, for evaporation *InAs* with help method molecular-beam epitaxy on *GaAs* substrate grown pyramidal phasons have alike sizes [12]. For temperature of substrate 460°C pyramid with quadratic basis is grown (side a = 12 *nm* and height h = 6 *nm*). These pyramids are equivalent to sphere with diameter ~ 8 *nm*. If process of evaporation was interrupted to achievement of optimal sizes by phason, then transition molecules to new phase centers is realized to achievement of optimal sizes by phason. If assume, that growth pyramids are *InAs* phasons, then value of energy of relationship to electron in *InAs* for temperature 460°C is w = 0,45 *eV*. This value is placed between values of energy of relationship for room temperature for *In* (w = 0,3 *eV*) and *As* (w = 0,8 *eV*), that explain observed results. Increasing of pressure of *As* vapor is caused the decreasing of value of basis of pyramid and it volume. Increasing of *As* concentration displacing w in side of it value for *As*, that is caused the decreasing of phason sizes.

On the basis of this conception, sizes of phasons of any materials may be estimated, if it relationship to electron is famous. Values of phasons sizes for basic technological elements, which estimated with help values of energy relationship to electron, have next meanings.

Elements – *d*, *nm*: Al – 7; Co – 4; Ni – 5,5; Mo – 3; Ag – 2,8; In – 12; Sn – 3,2; Au – 1,6; Si – 2,6; Cu – 2,9; Ge – 2,9; Sb – 3,3; Ga – 12; Te – 1,8; As – 4,5.

It is real values for phasons. For example, minimal size of tin drops, which fly from edge after action of strong electrical field [20] ~ 2 *nm*. In metal alloys [20] structural defects have analogous sizes: in Cu+Au – 1,5 *nm*, in Au+Pd – (2–3) *nm*, in Cu+Al – 2 *nm*, in Fe+Al – (4–5) *nm*. For evaporating in vacuum films Ti–Si–B–N [20] size of centers is 2–4 *nm*.

According to this model we can explain size and chemical composition of nanostructures, which are created after laser irradiation *GaAs* by pulse of second harmonic Neodymium-laser (Fig. 1) [8]. Pulse duration 15 ns.

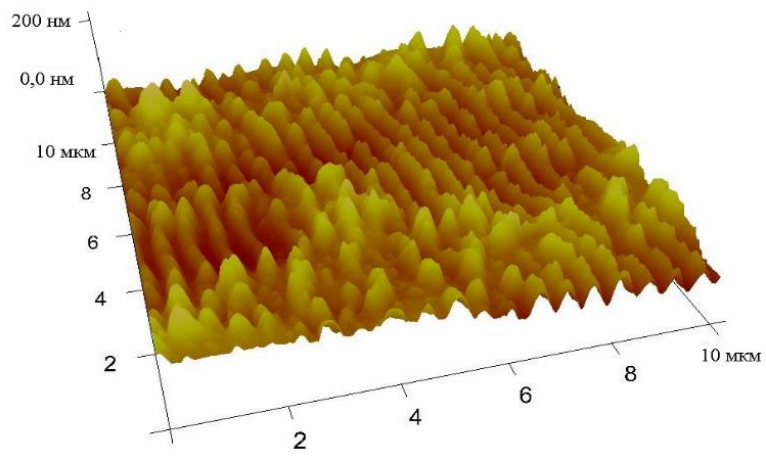

Fig1. *AFM 3D image of GaAs surface after irradiation by YAG:Nd laser at I=5.5 MW/cm² [8].*

The results from Fig. 1 may be explained in next way. Sizes of nanohills near basis are ~200 nm. This result is coordinated with estimations of sizes of crystallization centers according to cascade model [2]. However, according to Kapayev-Kopayev-Molotkov theory [4] and Prinsloo-Lee experimental data [4] arsenic atoms must be placed on the tops of nanohills. According to Stafeev model pure precipitate of arsenic has diameter 4,5 *nm*, therefore polyphazons, which is enriched of arsenic atoms, are created on tops of nanohills. Gallium phasons have sizes 12 *nm*, therefore it generation more possible near surface of crystal [2].

Ice phasons in water

Electrochemical potential of ice is less as in water [20], therefore ice phasons in water will have positive electrical charge.

For temperature 20°C junction difference of potentials ice and water is equaled 15 meV, therefore size of phason d_o = 3 *nm*, number of molecules 400 – 500. According to experimental data [12], water have fluctuation of density with minimal size 3 *nm*, that practically is corresponded to our estimation. According to [12] for temperature 0°C one electrical charge belong to claster with $3 \cdot 10^7$ water molecules, it correspond of phason size d_o = 100 *nm*. According to value εφ from [12] quantity d_o = 6,1 *nm* [12] much less from experimental, therefore estimated in [12] value of difference of electrochemical potentials in this thermal region is value-added. Naturally phasons may be united in multicharged polyphasons.

Water density ρ has maximal value for temperature ~ 4°C. It decrease for decreasing and increasing of temperature (Fig. 2).

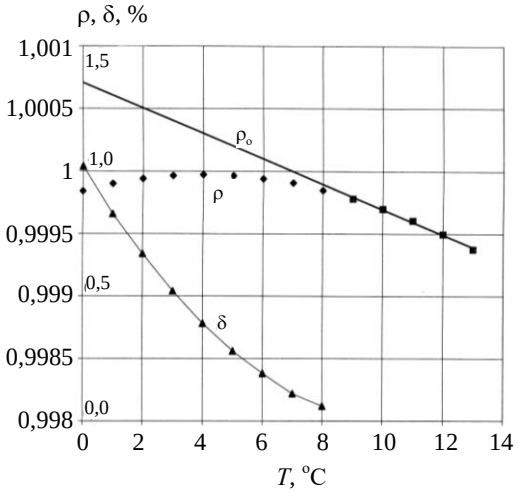

Fig2. *Dependence from temperature the water density ρ and part of ice-similar phase δ [12].*

Ice density ρ_l is less as water density, therefore increasing of quantity of water molecules in ice phasons will be compensate the increasing of density more thick phase. Thermal dependence of his thick phase may estimate with help extrapolation of the thermal dependence of water density from region of high temperatures, another words "normal" thermal dependency, in region of low temperature. In Fig. 2 it is represented the line ρ_o. Thermal dependency of density of ice centers ρ_l may be received with help extrapolation of ice density from region of low temperatures (less as 0°C). Part of ice-similar phase $\delta = (\rho_0 - \rho)/(\rho_0 - \rho_l)$.

Estimated with help of this method thermal dependency of part of ice-similar phase is represented in Fig. 2 (curve δ). It is lesser as estimating value in [12] and decreases with increasing of temperature.

For drawing to frozen temperature quantity and sizes of ice phasons are increased and its proportion for temperature 0°C is near one percent. Therefore, concentration of phasons with size d_o ~100 *nm* is equaled $N_f \approx 10^{13}$ cm^{-3}. A concentration of hydrogen ions for this temperature $-N_H = 1{,}8 \cdot 10^{13}$ cm^{-3}. So, near half hydrogen ions in water are included in phasons of ice centers.

In water after melting polyphasons of ice are existed in quantity, which is much large as in thermodynamical equilibrium state. It may be stipulated the special properties of melting water, which are disappeared after 15-20 hours [12].

Difference of electrical potentials that appear under phase transition water-ice firstly was investigated be Vorkman and Reynolds [12]. In pure distillated water between ice and electrode, which is placed on distance ~0,5 *cm*, difference of electrical potentials near to 60 *V* in water is observed, moreover ice charging positively. This difference is depended from type of dissolved ions and may be change sign from positive to negative. For example in water solution with $\sim 10^{-7}$ *M* NH_4SO_4 is appeared the difference of potentials more as 200 *V*. For dissolution *HCl* in water ice grasp only ions H^+. With increasing of concentrations of dissolved materials appearing difference of potentials is decreased. Next admission was made [12]: large electrical charging complexes are condensed on surface of layer growing ice. One ion is place in $3 \cdot 10^7$ water molecules.

According to model in [12], in process of freezing of water on cooling surface may be condensate charging ice phasons. Therefore, our surface is charged comparatively to water. Electrochemical potential of ice is less as pure water; therefore ice phasons and surface of ice have positive charge. When velocity of growing the ice layer is 1 μm/s and phason size – 100 *nm* 10^{11} single charged ice phasons are condenced on square 1 cm^2, that cause the appearance of electrical current $I = 10^{11}\ q/c = 1{,}6 \cdot 10^{-8}\ A$. This current is caused the generation of electrical field $E = I\sigma^{-1}$. In pure water $\sigma = 1{,}6 \cdot 10^{-8}\ (Ohm \cdot cm)^{-1}$, therefore generating electrical field has value $E \sim 1\ V/cm$; for ice $\sigma = 1{,}9 \cdot 10^{-10}\ (Ohm \cdot cm)^{-1}$, therefore $E \sim 80\ V/cm$.

Dissolved in water materials practically aren't grasped of ice clasters, therefore the difference of electrochemical potentials ice-water will be depend from type of dissolved impurity and its concentration. Accordingly, appearing on border of growing ice the difference of potentials will be depend from value pH of solution up to change of it sign.

Heat capacity. An appearance of ice phasons is accompanied of separation of energy of phase transition water-ice and of absorption of energy, which is necessary for the formation of charged polyphasons in water. It may be estimated from the comparison of value of heat capacity C_p near temperature 0°C and it extrapolated value with region of temperatures 15–20°C, in which role of ice phasons is neglicted (Fig. 3) [12].

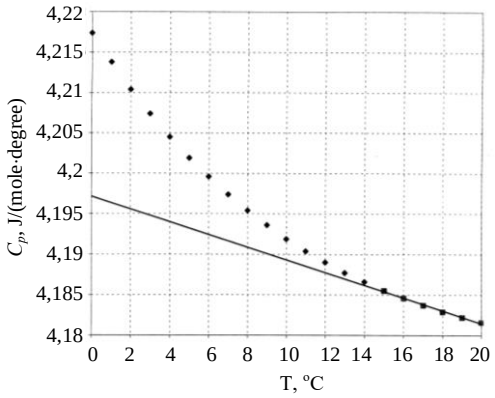

Fig3. *Dependence of heat capacity from temperature [12].*

Estimated additional heat capacity under temperature 0°C is equaled $\sim 2 \cdot 10^{-3}\ J/g \cdot grad$. Proper value of hiding heat of creation ice polyphasons in water is next

$$Q = \Delta C_p (\Delta\delta/\Delta T)^{-1}. \quad (1)$$

Under 0°C it is $\sim 2 \cdot 10^{-3}\ J/g \cdot grad$. Under 0°C $Q \sim 11$ J/g, in region of temperatures (3–7) °C $Q \sim 8{,}5$ J/g.

Thermoelectrical and electrogravitational effects [12]. Positive charged ice polyphasons in electrical field *E* are displaced from anodic region (region of it birth with separation of energy *Q*) to catodic region (region of it melting with absorption of energy *Q*). In this fielg energy $Q_f = \mu E \delta \rho_l Q S$ is transmitted. In stationary conditions heat flow is balanced of heat capacity $\lambda S dT/dx$, where λ – coefficient of heat capacity of water, *S* – square. Appeared thermal gradient $dT/dx \sim \mu E \delta \rho_l Q/\lambda$. Under $T = 0$°C thermal gradient is appeared in water $dT/dx \sim 4 \cdot 10^{-4} E$ K/*cm*, under temperature 8 °C it decrease approximately on order. Flow of polyphasons is formatted in water under presence in water thermal gradient, it create electrical current $qD\{\partial(mN_f)/\partial T\} \times dT/dx$, which is balanced of current of conductivity σE. Appeared electrical field $E = \{qD\partial(mN_f)/\partial T\}\sigma^{-1} dT/dx$.

In pure water under temperature ~0 ºC σ ~1,5·10^{-8} $(Ohm \cdot cm)^{-1}$, therefore $E \sim 4 \cdot 10^{-7} dT/dx$ *V/cm*, if conductivity is determined of phasons only then $E = (kT/q) \times \{\partial(mN_f)/\partial T\}(mN_f)^{-1} dT/dx$.

For location of cooling zone adown in gravitational field ice polyphasons in water are moved upwards, that is caused of appearance of difference of electrical potentials. It is electrogravitational effect.

Water phasons in air [12]. Energy of affinity to electron of molecules H_2O in air is equaled 0,9 *eV*, therefore water and ice phasons will be have negative charge. Under room temperature d_o~4 *nm*, μ~0,26 $cm^2/V \cdot s$. Near negative charged surface of Earth electrical field is equaled ~130 *V/m*. Negative charged polyphasons in this field must rise up against to gravitational force with velocity ~0,3 *cm/s*. It are hanged in air under sizes ~1 *μm* and charge ~250 *q*, that is corresponded to sizes of mist drops. Energy of affinity of molecule H_2O to proton H^+ *w* = 7,23 *eV*, therefore phasons of oxonium (H_3O) in air will be have positive charge, diameter ~0,5 *nm* and mobility ~2 $cm^2/V \cdot s$. In electrical field of Earth it be move down with velocity ~2,6 *cm/s*.

Electrical conductivity of dielectrical liquids is determined of own phasons [12]. Phasonic mechanism of electrical conductivity, unlike to ionic, isn't corresponded to irreversible chemical modifications. Phasons, which is carried charge, generating and without observing changes of material. Under ionic mechanism of conductivity to one charge is corresponded one "portable" molecule. Phasonic mechanism of run of current is accompanied the displacement of macroquantities of matter. Phason with one electrical charge is included hundreds, thousands and millions molecules. A creation of polyphasons is caused the increasing of quantity of materials, which is carried of unit electrical charge proportionally to square of number its charges. This fact is interpreted as change of step of dissociation of molecules.

In pure water near temperature of freezing a contribution of ice phasons in electroconductivity is 1% and hasn't observable value.

Luminary carrying of materials is realized under small electrical currents. A division of liquid on channels with liquids flows in opposite directions is realized after increasing current density. Charging phasons is moved in ones channels, basic part of liquid with opposite charge is moved in another channels in opposite directions.

After increasing of electrical field the velocity of polyphason motion is increased and flow is transformed to turbulence with creation of "curls". This phenomenon is corresponded to liquid crystals.

Liquid crystals. Basic peculiarities of phenomena in the region of phase transitions are clearly represented for liquid crystals [12].

Thermal dependence of current under stable electrical voltage 95 *V* is represented in Fig. 4a [12]. Centers of low temperature phase of cholesterylcaprylate in decan have more large density in comparative to liquid phase, therefore under cooling it lower after action of gravitational forces. Phasons are charged and its motion is caused the electrical current and appearance of difference of potentials with opposite polarity to applied voltage. In region of phase transition current flows against to external voltage.

In Fig. 4b) thermal dependence of "discharged" current that appear in layer under cooling (curve *a*, Fig. 4b*)* and after heating (curve b, Fig. 4b*)* without external voltage. In region of phase transitions strong surges of current are observed: under cooling in one side and under heating in opposite side.

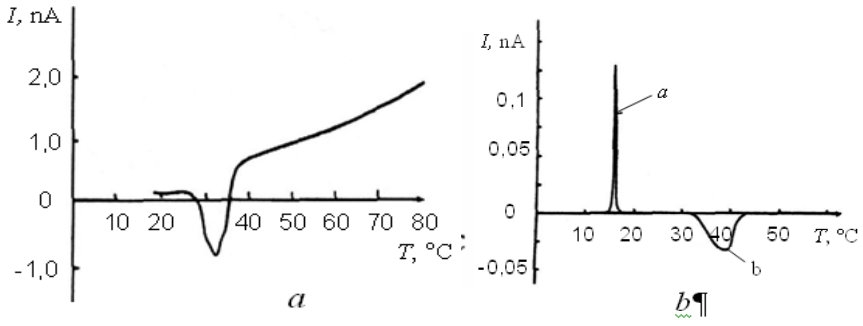

Fig4. *Thermal dependence of current: a – for stable external voltage 95 V; b – discharged under cooling and heating of layer EBBA [12].*

Phasons of low thermal phase are created and lowered in volume and it cause electrical current. Under increasing of temperature phasons of liquid phase are surfaced and caused electrical current of back direction. Full quantities of charges that created under cooling and heating are equaled approximately. Last result proofs the equivalence of phasons sizes. Under heating rate of creation is less because phasons are created on surface, but under cooling – in all volume of liquid phase. This fact is determined various forms of discharged curves.

Phasons of cholesterylcaprylate in 0,8*N* solution in decan hang under voltage 5 *V* in layer with depth ~1 *mm* [12]. According to these data relation of carrying charge to phason mass is equaled $2{,}5\cdot10^{-7}$ *C*/*g*. Thus size of phasons of this material in decan is $d \sim 1\ \mu m$. In region of phase transitions centers of low temperature phase are observed. It cause the scattering of light in visible spectral range – "blue" liquid crystals, another words phasons have sizes ~1 μm. Electric constant of decan $\varepsilon \sim 2$, therefore estimated value $\varphi \sim 2\ mV$, if growing centers are one-charged phasons.

In pure dialectical liquids own electroconductivity is determined of own phasons. In the region of phase transition quantity of phasons is increased sharply that explain the jumps of electroconductivity, viscosity and breach of Valden-Pisarzhevski law [12].

Photon crystals. Spherical particles of amorphous SiO_2 are created on the basis the reaction hydrolysis of tetraether of orthosilicon acid (tetraetaxilan $Si(OC_2H_5)_4$) in ethanol (C_2H_5OH) in presence of hydroxide of ammonia (NH_4OH) [12]. At first stage spherical particles with sizes ~5 nm are created, it format amorphous spherical particles with sizes in borders 200 – 600 *nm*. Standard size of particles is 260 *nm*. Average scatter is ~ 3 % [20].

Spherical particles SiO_2 with sizes ~5 nm is phasons of molecules SiO_2. On the sizes of spherical particles we can estimate the quantity $\varepsilon\varphi = 3{,}6/d_0 \sim 0{,}7\ mV$ under $\varepsilon = 1$ for phason of molecule SiO_2. Spherical particles, which are generated by phasons of molecules SiO_2, will be have the quantity $\varepsilon\varphi$ in corresponding times less, another words for $\varepsilon = 1$ $\varphi \approx 14\ mV$. Since $\varepsilon\varphi$ has small value therefore these large particles are formatted relatively slowly as phasons of fullerenes.

Phasons of biological objects. Any biological object is organic phase in proper environment. Under investigations of microobjects, including biological, we often postulate that these objects are electrical neutral [12]. But really in biological objects microcomponents have negative charge with number of carriers *q* to few tens [12]. These properties are used for its separation with help of method of electrophoreses.

Minimal biological objects are viruses. Minimal sizes are existed for various viruses: 24 *nm* (virus of tobacco mosaics), 28 *nm* (viruses of poliomyelitis, yellow mosaics of turnip a.o.). It have, as rule, spherical form. Therefore these viruses may be represented as elementary biological phasons with unitary electrical charge in environment with electric constant $\varepsilon = 1$. Under it sizes we can estimate energy of affinity of viruses– $w \sim 130–150\ meV$. A Relationship to proton of organic molecules is equaled few electron-volts, which is corresponded of size of separate little molecules, another words much less as size of virus. Therefore, energy of affinity of viruses is relationship to electron and viruses in air must have negative charge.

Biological objects with size to 1 μm must be charged negatively and carried charge of few decathlons *q*, these results are observed experimentally [12].

For room temperature virus mobility in air $\mu \sim 0{,}04\ cm^2/V{\cdot}s$, diffusive coefficient $D \sim 10^{-3}\ cm^2/s$. Near to surface of Earth electrical field is equaled ~130 *V*/*m*, therefore viruses will be move to up from it surface with velocity 1,5 *m*/*hour*. It is favored of some clearance of lower layers of atmosphere from biological and other microobjects with sizes less as few hundreds nanometers. It go to cosmos and decrease it negative charge.

Electrical currents. Since all objects are charged therefore it motion must be accompanied of electrical current and appearance of proper magnetic field.

Biologic object with size ~10 *cm* will be carried electrical charge $10^{-12}\ C$ in air. Under motion with velocity (30-40) *km*/*hour* a flock with thousands of these objects is created electrical current ~1 μA. Existing electromagnetic field is performed regulative role under motion of flock.

A blood has charge relatively to walls of blood vessels, therefore it flow must be perfomed of electrical current and proper electromagnetic field. Respectively external magnetic field must be acted on blood flow and motion of its microparticles (erythrocytes a.o.). May be it cause to magnetic- and meteosensitivity of peoples and other living organisms.

Electrochemical potentials of water and surrounding of it coasts are various, therefore on its borders junction difference of potentials are existed that depend from PH water. Water must be charged. Therefore current of river, including underground, must accompany of electromagnetic field. May be exactly electromagnetic field of underground water flows allow to search it by help of dowsers.

Water surface must be charged relatively to air. Surface density of electrical charges is 10^{-9} C/m^2. Therefore waves and flows of water must generated electromagnetic fields. Exactly warm currents as Holfstrem, Kurosivo a.o. [12] are charged relatively to surrounding cooler environment. Therefore these colossal flows are surrounded of electromagnetic field. Flows of sea water, which are caused with rotation of Earth and attraction of Sun and Moon, must surround of electromagnetic field too.

Great quantity of dusting particles is fallen on Earth from cosmos. Since it must be charged therefore these flows are surrounded of electrical current and proper electromagnetic field. It must influence on atmosphere phenomena.

Plasma crystals [12]. In free environment materials may have forms of atoms, molecules, clusters and as particles of condensed matter phase. In generally this set of particles must be neutral. If it is consisted with various materials or various phases, then its components must be electrical charged because these components have various quantity of relationship to electron (proton) or various electrochemical potentials. This set of particles and molecules is created quasineutral plasma. Phasons in free “cool” dusting plasma are charged and in some conditions can format similar to crystal structures with lattice number, which is caused of electrical charges of phasons of this material. Now we have “plasmic crystals”. For example in [12] "dusting plasma" was formatted from spheres of borosilicon glass with sizes 50-63 μm and estimated electrical charge ~$7 \cdot 10^5 q$. Elementary one-charged phason of this material must be have size ~1 nm and quantity φ ~ 4-5 V. These phasons were created ranked structures with lattice number ~300 μm.

Dusting clouds in cosmic space are consisted from particles with little sizes. It must be electrical charged; therefore, external electrical and magnetic fields must be influenced on proper phenomena. It is related to dusting tails of comets too.

Thus Vitaliy Stafeev theory of phasons is “electrostatic” addition to other theories of nucleation [12].

2.2. Cascade models of step-on-step excitation of proper chemical bonds in the regime of saturation the excitation

The profiles of the distribution the photostimulated donor centers in subsurface layers InSb and *InAs* are represented in Fig. 5 [3].

The samples of p-type conductivity are irradiated. For intensity of irradiation $I_0 > 0{,}01$ $J \cdot cm^{-2}$ for *InSb* and $I_0 > 0{,}012$ $J \cdot cm^{-2}$ for *InAs* the n-layers on p-type materials are created. For intensity of irradiation $I_0 < 0{,}1$ $J \cdot cm^{-2}$ for *InSb* and $I_0 < 0{,}16$ $J \cdot cm^{-2}$ for *InAs* the profiles of the distribution of donor centers are represented the Buger-Lambert law (law of absorption the light in homogeneous media). For further increasing the irradiated intensity the profiles of the concentration donor centers have diffusion nature. The visible destruction of the irradiated semiconductor melting, the change of the surface color) had place for $I_0 > 0{,}3$ J·cm^{-2} for *InSb* and $I_0 > 0{,}5$ $J \cdot cm^{-2}$ for *InAs*. This effect has oriental character (Fig. 6) [4]. For crystallographic direction {111} the process of the creation damages is more effective as for direction {110}.

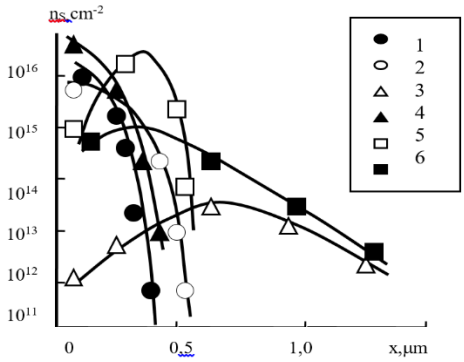

Fig5.*The profiles the distribution the layer concentration of the donor centers in inverse layers InSb and InAs after ruby laser irradiation with various density of energy (monoimpulse regime): 0,07 (1); 0,1 (2); 0,16 (3); 0,16 (4); 0,25 (5); 0,5 J·cm^{-2} (6). 1-3 – InSb, 4-6 – InAs [3].*

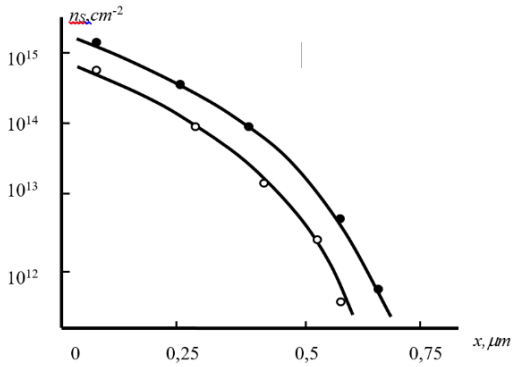

Fig6. *The oriental effect of the creation ruby laser stimulated damages in InSb:– {111}; - {110};* I_0 *=0,1 J·cm*$^{-2}$ *[3].*

Analogous results were received for the indium arsenide too. Time and energy characteristics of processes on Fig. 5 may be estimated with the help of next way. In further we'll use two-dimensional representation of crystal lattice *InSb* (Fig.7). Bond 1 is corresponded to band gap and has value 0,18 *eV*, bond 2 – 1,95 *eV* and bond 3 – 2,15 *eV* [3]. For *InAs* bond 1 has value 0,36 *eV*, bond 2 – 3,8 *eV* and bond 3 – 4,2 *eV* [3].

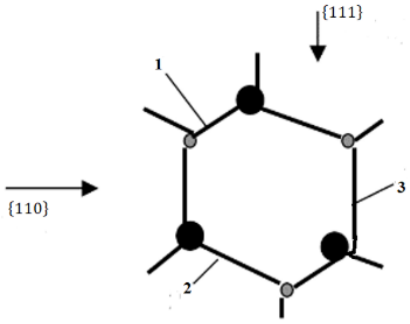

Fig7. *Two-dimensional picture the crystal lattice* A_3B_5 *(including InSb and InAs) the cubic symmetry. Bond 1 is pure covalent [3].*

Method of the estimation of level of saturated excitation of proper chemical bonds may be used for the selection of optimal regime for optical pumping of semiconductor laser [3] and for creation stable *n–p*-junctions on semiconductors [3] and for the creation layers with new phases, including nanostructures [3].

For these crystals the energy of these bonds are equaled the energy of band gap E_g (0,18 *eV* for *InSb* and 0,36 *eV* for *InAs* at room temperature). On Fig. 7 this bond is signed as 1. For this bond ions *In* and *Sb* (or *In* and *As*) are placed on minimal distance (the sum of proper covalent radiuses). Other chemical bonds in this crystal symmetry have more long sizes. With geometrical point of view in crystal direction {111} the cross section of effective interaction the light quantum with bond 1 is more effective than for direction {110}. The angle among bond 1 and direction {110} is 37,5°. Quanta of ruby laser in linear regime of the irradiation are not interacted with another bonds practically because it energies are less than energy of this bond. The correlation of effective square of bond 1 for directions {110} and {111} is explained the proper experimental data (oriental effect of creation donor centers see Fig. 6).

Energy density, which was required for the excitation of "band gap" bonds, is equalled

$$E_1 = 2h\nu \frac{3}{4\pi r_k^3}, \tag{2}$$

factor 2 is included the large reflection of irradiation from surface of indium antimonite. For *InSb* $E_1 = 8.6\ {}^{J}/_{cm^3}$. Next phase of excitation is the ionization second valence bonds with energy 1,95 *eV* (for two-dimensional representation of crystal lattice *InSb*, Fig. 7). With including first processes $r_{k_2} \approx 0.45\ nm$ for our second process. Therefore,

$$E_2 = 2h\nu \frac{3}{4\pi r_{k_2}^3} \tag{3}$$

For *InSb* $E_2 = 1510 {}^{J}/_{cm^3}$. After including the depth of irradiated layer (from 0,2 μm to 0,6 μm) the diapason of change energy intensity is next: from $E_{1s} = 8.6 \cdot 10^{-5} {}^{J}/_{cm^2}$ to $E_{2s} = 0.03 {}^{J}/_{cm^2}$. Further increasing of intensity the radiation lead to the ionization third valent bond with energy 2,15 *eV*. The regime of saturation of its excitation lead to the melting of irradiated semiconductor. For the *InSb* this value is $E_{3s} = 0.16 {}^{J}/_{cm^2}$.

Straight method of the estimation the energetic characteristics this processes may be realized in the next way. Energy of "disruption" of chemical bonds of one type is equalled

$$E_{di} = N_i E_i, \tag{4}$$

where N_i – a density of proper bonds; E_i – energy of a disruption (ionization) one bond.

For the *InSb* $N_1 = N_2 = N_3 = {}^{N_0}/_{2}$ and are equaled $1.4 \cdot 10^{22} cm^{-3}$, $E_1 = E_g = 0.18\ eV$ and therefore $E_{d1} = N_1 E_g = 403.2 {}^{J}/_{cm^3}$ and $E_{d2} = N_2 E_2 = 4368 {}^{J}/_{cm^3}$. Surface density of irradiation may be determined with the help of next formula [3, 4]

$$E_{sis} = \frac{E_{di}}{\alpha_i}, \tag{5}$$

where α_i – proper absorption factor, for the first bonds of *InSb* $\alpha_1 = 2 \cdot 10^5 cm^{-1}$, for second – $\alpha_2 \sim 10^5 cm^{-1}$. Second absorption factor is nonlinear and take into account the effect of blooming. For *InSb* these values are next E_{s1s} =0.002 ${}^{J}/_{cm^2}$ and E_{s2s} =0.04368 ${}^{J}/_{cm^2}$. These values must be multiplied on 2 (with including reflection) and therefore real values are next E_{s1sr} =0.004 ${}^{J}/_{cm^2}$, E_{s2sr} =0.08797 ${}^{J}/_{cm^2}$ and $E_{\Sigma r(2)} \approx 0.092 {}^{J}/_{cm^2}$. Energy of "disruption" of third chemical bonds (Fig.4.4) is equaled $E_{d3} = N_3 E_3 = 4816 {}^{J}/_{cm^3}$. If $\alpha_3 \sim 10^5 cm^{-1}$ we have E_{s2s} =0.04816 ${}^{J}/_{cm^2}$ and E_{s3sr} =0.096 ${}^{J}/_{cm^2}$. Summary surface density of energy of three bonds is equaled $E_{\Sigma r(3)} \approx 0.188 {}^{J}/_{cm^2}$. Value $E_{\Sigma r(2)} \approx 0.092 {}^{J}/_{cm^2}$ is represented of curve 2 on Fig. 5 and $E_{\Sigma r(3)} \approx 0.188 {}^{J}/_{cm^2}$ – curve 3 on Fig. 5.

Large difference between estimations of cascade and straight methods is caused of neglect or real geometry of "photon" zone and the disruption of "selected" bonds only. But cascade approximation may be used for the estimation of process of the formation wave zone. An eclipse of "photon" zones is the beginning of the formation wave zone. Practically minimal value $E_{1sr} = 8.6 \cdot 10^{-5} {}^{J}/_{cm^3}$ for *InSb* is the threshold for the formation of various electromagnetic wave oscillations, including plasmic. This value may be represented as maximal value of optical pumping for the receiving laser generation with $h\nu = E_g = 0.18\ eV$ in *InSb* and $E_g = 0.36\ eV$ in *InAs*. For *InAs* $E_{1srInAs} \sim 1.8 E_{1srInSb}$[3].

It should be noted that light absorption mechanisms play an important role in the formation of crystalline phases. Thus, the irradiation of unalloyed antimonite and indium arsenide with the radiation of a pulsed neodymium and ruby laser leads to the formation of donor layers and a decrease in the symmetry of the starting material. Therefore, this radiation is not suitable for annealing ion-implanted layers of these materials [3, 28].

The fact is that this radiation leads to phase modifications of the pure material. The use of CO_2 laser radiation leads to annealing of defects and crystallization of ion-implanted layers. Moreover, the irradiation modes (impulse or stationary) do not matter, the main role is played by the integral dose. That is, in this case, we have photochemical processes [3].

Now we show the using of cascade model for the explanation experimental data of laser-induced phase transformations in silicon, germanium, carbon and titanium. It was called as case the structural phases [1].

The question about the influence of saturation of excitation on effects of RO may be represented as process of transitions between stable and metastable phases too. Now we'll estimate the influence of

parameters of irradiation (including spectral) on irreversible changes and transformations in *Si* and *Ge*. Spectral dependences of absorbance of various structural modification of *Si* are represented in [1-5]. Now we'll be estimated intensities of eximer, Ruby and Neodymium laser irradiation (wavelengths of irradiation are 0,248 μm, 0,69 μm and 1,06 μm properly of silicon and germanium, which are necessary for the creation of proper irreversible changes in irradiated semiconductor. As shown in [97], absorbance of the Neodimium laser radiation in silicon is equaled 100 cm^{-1}, second harmonic of Neodimium laser – 10^4 cm^{-1}, eximer laser – 10^6 cm^{-1}.

Crystal semiconductors *Si* and *Ge* have, basically, the structure of diamond. Volume atomic density of elementary lattices may estimate according to formula [11]

$$N_a = \frac{\rho N_A}{A}, \tag{6}$$

where ρ – density of semiconductor, N_A – Avogadro number, A – a weight of one gram-atom. For *Si* $N_{aSi} = 5 \cdot 10^{22} cm^{-3}$, and for *Ge* $N_{aGe} = 4.4 \cdot 10^{22} cm^{-3}$.

But *Si* and *Ge* may be crystallized in lattices with hexagonal, cubic, trigonal and monoclinic symmetry. Phase diagram of Si as function of coordination number is represented on Fig. 8 [10].

Coordination number (CN) 8 is corresponded of diamond lattice, CN 6 – hexagonal lattice, (CN) 4 and (CN) 3 – other two lattices. It should be noted that melting temperatures of these phases are various. Volume density of CN is equaled CN·N_a. For diamond symmetry of lattice this value is 8N_a. In other words, a change in the coordination number is not necessarily related to a change in type of crystal syngony. Thus, the coordination numbers 8 and 6 can correspond to two different cubic symmetries, and at the same time, CN 6 corresponds to hexagonal syngony [29], which corresponds to the corresponding experimental data [1, 3].

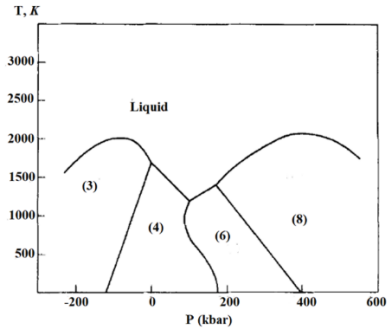

Fig8. *A schematic phase diagram for Si(CN). The coordination numbers (CN) of the various phases are indicated. The diagram is based on common features of the phase diagrams of column IV elements as described by the references cited in Pistorius's review (Ref. 8 in [10]). Starting from a high temperature >3□10^{3}K and subject to a constraint of average density $\langle\rho\rangle = \rho(4)$, a hot micronucleus will tend to bifurcate into the most stable phases (highest T_m) which straddle Si(4) in density. These are Si(3) and Si(8), as indicated by the diagram [10].*

Roughly speaking, transition from one phase to another for regime of saturation of excitation may be modeled as one-time breakage of proper numbers of chemical bonds, which are corresponded to the difference of CN of proper phases. For example, two bonds breakage is caused the phase transition from diamond to hexagonal structure. One bond breakage in the regime of saturation is caused to generation of laser radiation.

Results of calculation of volume densities of energy, which are necessary for breakage of proper number of bonds in regime of saturation of excitation, are represented in Table 1. [3]

Table1. *Volume density of energy I_{vi} (10^3 J/cm^3), which is necessary for the breakage of proper number of chemical bonds in the regime of saturation of excitation in Si and Ge.*

	I_{v1}	I_{v2}	I_{v4}	I_{v5}
Si	12,8 – 14,4	25,6 – 28,8	51,2 – 57,6	63 – 72
Ge	6,3 – 8,4	12,6 – 16,8	25,2 – 33,6	31,5 – 42

It conceded that energies of all chemical bonds for elementary lattice are equivalent (*Si* and *Ge* are pure homeopolar semiconductors) [28]. For silicon energy of covalent bonds *Si-Si* are equaled 1,2–1,8 *eV*; for germanium energy of covalent bonds *Ge–Ge* are equaled 0,9–1,6 *eV* [2, 4]. Minimal values of these

energies are corresponded of Pauling estimations. These values are corresponded the energy on one CN: according to radiation physics of status solid Zeits energy of creation one radiation defect in silicon is equal 12,7 eV for diamond lattice [28].

Surface density of energy on proper numbers of CN for proper lasers irradiation may receive after division of results of Table 1 on proper absorbance. This procedure allows to transit from bulk to surface density of energy, which is necessary for the receiving of proper phenomena. Results of these calculations are represented in [1, 3].

It should be noted that real regimes of irradiation must be more (process of light reflection wasn't included in our estimations). In addition we aren't include the relaxation (time) processes for the scattering of light on stable centers (self-absorption in crystals) as for *InSb* and *InAs* [3]. For physical-chemical modeling of phase transformations in irradiated materials, it is possible to use such quantities as the energies of formation of the corresponding crystal lattices and their volumes.

The lack of study of other crystallographic modifications of silicon compared to the diamond structure is due to the fact that the electronic and optoelectronic industry uses cubic modification and more complex methods of obtaining by more trivial methods of crystallization.

It is also important to estimate the corresponding energies of crystal lattices. Calculation according to the phase diagram Fig. 8 was taken from the value of the energy of defect formation for silicon and germanium. Then it was divided by the coordination number and we got the energy corresponding to one configuration number. This model made it possible to explain the nature of the appearance of hedgehog-like structures on silicon by series of nanosecond pulses with a wavelength of 248 nm [13, 14] and femtosecond pulses with a wavelength of 800 nm [15]. According to the estimates in Table 1, there is a cascade of structures (from bottom to top): cubic, hexagonal, and triclinic symmetry [1, 3] or other crystal modification. In this way, we can find out the energy difference per atom in different lattices of crystallographic lattices. The disadvantage of this method is that we assume that all bond energies are the same, which is only true for a diamond-type lattice.

It should be noted that the methods of calculating the energies of defect formation, as well as the energies of the crystal lattice, give certain scatters in the results. So, for example, the value of the energy of defect formation for silicon for a diamond lattice is equal to the sum of eight energies of covalent chemical bonds according to L. Pauling [1-5].

Modeling the change in the number of coordination numbers is a rather complex problem. Since, if in the diamond modification all bond energies are the same, then in other crystallographic modifications this is not the case. Therefore, for more precise calculations, we must use energies of corresponding real crystal lattices [22].

3. SOME REMARKS

Lattice energy – the energy (U) spent on breaking the crystal lattice into its components with the transfer to the distance of the absence of interaction, taken with the opposite sign. If the lattice is ionic, then this is the energy of rupture into the corresponding ions; if atomic or molecular, then this is the energy of rupture into atoms, molecules, etc. for molecular lattices, this is only a small part of the bond energy in the lattice, since the bonds of atoms inside molecules do not enter into it. Energy of crystal lattice for molecular lattices is equal to the van der Waals forces (see Chemical van der Waals bond). It has now been established that abs. most natural compounds, in particular oxygen ones, are not ionic, but at best semi-ionic and semi-covalent. In this regard, many conclusions based on the use of energy the crystal lattice, usually calculated as ionic ones, are of little value [22]. There are a number of methods for calculating energy the crystal lattice for binary compounds: according to the Born-Haber circular process, according to the Born-Lande formula and its simplified variants – the Kapustinsky formulas, etc.

According to the circular process [22]

$$U_i = Q + S + D + I - E, \tag{7}$$

where U_i is the energy of the ionic lattice; Q is the heat of formation, S is the heat of sublimation, D is the dissociation energy, I is the ionization energy, and E is the electron affinity energy. According to the Born-Lande formula [22]

$$U_i = \frac{aW_1W_2Ne^2}{R}\left(1 - \frac{1}{m}\right), \tag{8}$$

where a is the Madelung constant, W_1 and W_2 are the ion valences, R is the interatomic distance, Ne^2 is the product of the Avogadro number and the elementary electron charge squared, m is the coefficient. repulsion of electron shells. In geological sciences usually use the Kapustinsky formula [22]

$$U_i = 256.1 \frac{E_n W_k W_a}{r_k + r_a}, \quad (9)$$

where E_n is the number of structural units. W_k and W_a are the valencies of the cation and anion, rk and ra are their radii, or an even more simplified Fersman formula [22]

$$U_i = 256.1(E_c A + E_c B + \cdots + E_c X), \quad (10)$$

which has a universal character in terms of the values of E_k, which make up the compounds of ions, i.e., in terms of energy coefficient of components the calculation of energy the crystal lattice.

For atomic compounds, the circular process is simplified [22]:

$U_{at} = Q + S + D$,

for molecular compounds: $U_m = S(AB)$, where $S(AB)$ is the energy of sublimation of molecules. For the theoretical calculation, the formula is used where k is a coefficient, similar to the coefficient. Madelung, μ is the dipole moment. Idea about energy the crystal lattice plays an important role in the geoenergetic analysis of geochemical processes, so the correct use of this concept is very important.

Methods of Vitaliy Stafeev phason and cascade models complement thermodynamic methods and allow more adequately to include the microscopic aspects of the nucleation and crystallization.

Laser-induced crystallization and crystal growth are observed in [30]. Femtosecond multiphoton excitation of solutions leads to their ablation at the focal point, inducing local bubble formation, shockwave propagation, and convection flow. This phenomenon, called “laser microtsunami” makes it possible to trigger crystallization of molecules and proteins from their supersaturated solutions. Femtosecond laser ablation of a urea crystal in solution triggers the additional growth of a single daughter crystal. Intense continuous wave (CW) near infrared laser irradiation at the air/solution interface of heavy-water amino acid solutions results in trapping of the clusters and evolves to crystallization. A single crystal is always prepared in a spatially and temporally controlled manner, and the crystal polymorph of glycine depends on laser power, polarization, and solution concentration. Upon irradiation at the glass/solution interface, a millimeter-sized droplet is formed, and a single crystal is formed by shifting the irradiation position to the surface. Directional and selective crystal growth is also possible with laser trapping.

It should be noted that when laser radiation is focused in a transparent medium, the following cascade of processes may occur: focusing, diffraction stratification of the beam, Cherenkov radiation, and interference of this Cherenkov radiation [1, 2].

These processes can occur in all media from gases to solids. It is on the basis of the cascade of these processes that the laser-induced optical breakdown in silicon carbide and potassium chloride was explained. The same model can be used to explain the laser-induced growth of crystals from solution. It is the generation of Cherenkov (continuous cone) radiation that complements the tsunami effect from a physicochemical point of view, which allows breaking the corresponding chemical bonds, which in turn leads to both the creation of new molecules and a change in their phase state, that is, to crystallization.

Moreover, this can happen without interference, the main thing is the formation of short-wave radiation, which is absorbed more intensively than the incident radiation [2].

4. Conclusions

1. The problem of electromagnetic modelling the nucleation and crystallizations processes are is analyzed.

2. Short review of elionic methods of generation the nano- and microstructures is represented.

3. Vitaliy Stafeev electrostatic model of phasons as example of kinetic model of nucleation and its applications is observed.

4. It was shown, that cascade model of excitation of proper chemical bonds for two-dimensional sphalerite lattice may be used for the explanation the electrical properties of the laser-induced structures.

5. For structural modeling of transitions between allotropic phases of silicon and germanium and creation of proper nucleations was used its phase diagram.

6. Cascade model of step-by-step excitation the chemical bonds in the regime of saturation the excitation allows explaining main structural phase transformations in laser-irradiated matter.

7. For physical-chemical modeling of phase transformations in irradiated materials, it is possible to use such quantities as the energies of formation of the corresponding crystal lattices and their volumes.

8. Prospects for the development of electromagnetic modeling methods and the expansion of their field of application are also discussed.

ACKNOWLEDGEMENTS

Author wishes to thank by M. Romanyuk, Ya. Dovhyy, L. Laz'ko, A. Tsaryk, A. Krochuk, O. Vlokh, Yu. Denysyuk, I. Stoyanova, V. Stafeev, P. Eliseev, V. Bonch-Bruevich, Yu. Klimontovich, P. Danylchenko, F. Zaitov, A. Medvid and V. Makin for the discussion of basic questions and problems of coherence; and L. Sörensen, M. Shevchuk and D. Shvalikovskyy for help in the preparation of this work.

REFERENCES

[1] Trokhimchuck P. P. (2020) Relaxed Optics: Modelling and Discussions. Lambert Academic Publishing, Saarbrukken

[2] Trokhimchuck P. P. (2022) Relaxed Optics: Modelling and Discussions 2. AkiNik Publishing, New Dehly

[3] Trokhimchuck, P. P. (2016) Relaxed Optics: Realities and Perspectives. Lambert Academic Press, Saarbrukken

[4] Trokhimchuck P. P. (2020) Role Physical-Chemical Processes in the Generation of Laser-Induced Structures. In: Research Trends in Chemical Sciences, ed. Ashok Kumar Acharya, vol. 11, ch.6. AkiNik Publications, New Delhi, 109-140.

[5] Trokhimchuck P. P. (2022) Saturation of Excitation and Critical Processes in Nonlinear and Relaxed Optics. In: Recent Review and Research in Physics. Ed. Jayminkumar Rajanikant Ray, S. S. Sharma, vol. 1, ch. 3. AkiNik Publications, New Dehly, 69-98.

[6] Bogatyryov V. A., Kachurin G. A. (1977) The creation low resistively n-layers on *InSb* with help the impulse laser irradiation.Physics and technical of semiconductors, vol.11, No.1, 100-102. (In Russian)

[7] Höhm S., Rosenfeld A., Krűger J., Bonse J. (2012) Femtosecond laser-induced periodic surface structures on silica. Appl. Phys., vol. 112, Is.1, 014901-1 – 014901-9.

[8] Medvid' A. (2010) Nano-cones Formed on a Surface of Semiconductors by Laser Radiation: Technology, Model and Properties. In: Nanowires Science and Technology, ed. Nicoletta Lupu. Vukovar: Inech, 61–82.

[9] Grigonis A., Medvid A., Onufrijevs P., Jabonas J., A Reza A. (2008) Graphitization of amorphous diamond-like carbon films by laser irradiation. Optical Materials, Vol. 30, 749-752.

[10] Philips J. C. (1981) Metastable honeycomb model of laser annealing. Journal of Applied Physics, Vol. 52, No.12, 7397–7402.

[11] Baranskyy P. I., Klochkov V. P., Potykevich I. V. (1975) Semiconductor electronics. Reference book. Naukova Dumka, Kyiv (In Russian)

[12] Stafeev V. I. (2005) Elementary structural units of condenced phases and its proper electrical phenomena. Applied Physics, No.4, 31–38. (In Russian)

[13] Pedraza A. J., Fowlkes J. D., Lowndes D. H. (1999) Silicon microcolumn arrays growth by nanosecond pulse laser irradiation. Appl. Phys. Lett. 74(10), 2222-2224.

[14] Pedraza A. J., Guan Y. F., Fowlkes J. D., Smith D. A., Lowndes D. H. (2004) Nanostructures produced by ultraviolet laser irradiation of silicon. I. Rippled structures. J. Vac. Sc. @ Techn. B., Vol. 22, is.10, 2823-2835.

[15] Shen M., Carey J. E., Crouch C. H., Kandyla M., Stone H. A., Mazur E. (2008) High-density regular arrays of nanoscale rods formed on silicon surfaces via femtosecond laser irradiation in water.// Nanoletters, vol. 8, is. 7, 2087-2091.

[16] Tsukamoto M., Asuka K., Nakano N., Hashida M., Ratto M., Abe N., Fujita M. (2006) Period microstructures produced by femtosecond laser irradiation on titanium plate. Vacuum, vol. 80, 1346-1350.

[17] Donachie M. J. (2000) Titanium: A Technical Guide. Materials Park, Ohio

[18] Makin V. S. (2013)Peculiarities of the formation the ordered micro and nanostructures in condensed matter after laser excitation of surface polaritons modes. D. Sc. Thesis. State university of information technologies, mechanics and optics, Saint-Petersburg (In Russian)

[19] Fedosyuk V. M. (2006) Nanostructural films and nanowires. Belorussian University Press, Minsk (In Russian)

[20] Khaybullin I. B., Smirnov L. S. (1985) Pulse annealing of semiconductors. The state of the problem and unresolved questions (Review). Physics and technical of semiconductors, v.19, No.4, 569-589 (In Russian).

[21] Kurbatov L. N., Stoyanova I. G., Trokhimchuck P. P., Trokhin A. S. (1983) Laser annealing of semiconductors $A_{III}B_{V}$. Reports of Soviet Academy of Science, Vol. 268, No.3, 1983: 594–597 (In Russian)

[22] Dowty E. (1980) Crystal Growth and nucleation theory and the numerical simulation of igneous crystallization. Chapter 10. Physics of Magmatic Processes, edited by R.B. Hargraves. Princeton: Princeton University Press, N.J., 1980: 419-485.

[23] Okada T., Tomita T., Matsuo S., Hashimoto S., Ishida Y., Kiyama S., Takahashi T. (2009) Formation of periodic strain layers associated with nanovoids inside a silicon carbide single crystal induced by femtosecond laser irradiation. J. Appl. Phys., v. 106, p.054307, 2009. – 5 p.

[24] Okada T., Tomita T., Matsuo S., Hashimoto S., Kashino R., Ito T. (2012) Formation of nanovoids in femtosecond laser irradiated single crystal silicon carbide. Material Science Forum , vol. 725, 19 – 22.

[25] Paschotta R. (2008) Encyclopedia of Laser Physics and Technology, 2 Volume Set. John Wiley@Sons, New York, London a.o.

[26] Vorobyov A.Ya., Guo Ch. (2007) Effects of nanostructure-covered femtosecond laser-induced periodic surface structures on optical absorptance of metals. Appl. Phys. A, Vol. 86, is. 3, 321–324.

[27] Trokhimchuck P. P. (2021) Modelling of the elionic-induced sputtering (sublimation) of matter. Applied Questions of Mathematics modeling. Vol. 4. No. 2.1, 234-244.

[28] Trokhimchuck P. P. (2007) Radiation Physics of Status Solid. Lesya Ukrainka Volyn University Press "Vezha", Lutsk (In Ukrainian)

[29] Boky G. B. (1971) Crystal chemistry. Nayka, Moscow (In Russian)

[30] Sugiyama T., Masuhara H. (2011) Laser-Induced Crystallization and Crystal Growth. Chemistry – An Asian Journal. Vol. 6, is. 11, 2878–2889.

Citation: *Petro P. Trokhimchuck (2023) "Some Electrodynamics Problems of Modelling the Nucleation and Crystallization" International Journal of Advanced Research in Physical Science (IJARPS) 10(3), pp.19-34, 2023.*